Variability in noise-driven integrator neurons

R. Guantes*
Instituto de Matemáticas y Física Fundamental, Consejo Superior de Investigaciones Científicas, Serrano, 123, 28006 Madrid, Spain

Gonzalo G. de Polavieja†
Departamento de Física Teórica, C-XI, and Instituto "Nicolás Cabrera," C-XVI, Facultad de Ciencias, Universidad Autónoma de Madrid, Cantoblanco, 28049 Madrid, Spain
(Received 23 July 2004; revised manuscript received 24 September 2004; published 27 January 2005)

Neural variability in the presence of noise has been studied mainly in resonator neurons, such as Hodgkin-Huxley or FitzHugh-Nagumo models. Here we investigate this variability for integrator neurons, whose excitability is due to a saddle-node bifurcation of the rest state instead of a Hopf bifurcation. Using simple theoretical expressions for the interspike times distributions, we obtain coefficients of variation in good agreement with numerical calculations in realistic neuron models. The main features of this coefficient as a function of noise depend on the refractory period and on the presence of bistability. The bistability is responsible for the existence of two different time scales in the spiking behavior giving an antiresonance effect.

DOI: 10.1103/PhysRevE.71.011911 PACS number(s): 87.19.La, 02.50.Ey

Neurons are an important class of excitable dynamical systems, wherein a perturbation of an equilibrium (quiescent) state may be amplified to produce a large excursion of the relevant dynamical variables before returning to equilibrium. In neurons, this amplified response is due to the fact that ionic conductances depend on the membrane potential. This translates into sudden increases of the membrane voltage or spikes, which constitute the basic information units of the neural code. An important step towards the unraveling of this code is the understanding of how individual neurons respond to a given stimulus and which is the intrinsic dynamics responsible for this behavior.

From a dynamical systems perspective, the reason for excitability is that the neuron is close to a bifurcation point where a transition takes place between a rest state (a stable fixed point) and repetitive firing (a stable limit cycle) [1]. Obviously, how close the system must be to this transition point to be excitable depends on the particular case and the size of the perturbation. Real neurons are in general high-dimensional, nonlinear dynamical systems, where the number of dynamical variables is determined by the different kinds of ionic channels across the membrane contributing to spike generation. It is thus intriguing that, in spite of the large variability of ionic currents and conductances, all biophysically detailed neuron models can be grouped in two classes according to their excitable properties [1]. Historically [2], type I excitability is characterized by spikes generated with arbitrarily low frequency as a dc current is injected, while for type II neurons the onset of repetitive firing is at nonzero frequency. Moreover, for this last class the spiking frequency is relatively insensitive to changes in the applied current. From the point of view of dynamical systems theory, neurons are better classified as resonators or integrators [1], depending on two different dynamical scenarios: in resonator neurons, like the Hodgkin-Huxley model of the squid axon, repetitive firing is produced by a Hopf bifurcation where the only equilibrium point (rest state) loses stability as the current increases and the system falls on to a stable limit cycle. By contrast, integrator neurons have three equilibria for currents below the critical current, one of them for high voltage (stable or unstable), another stable for low voltage (a node), and another unstable with only one positive eigenvalue (a saddle point), see Fig. 1. At the critical value of current, these two last fixed points merge and disappear through a saddle-node bifurcation, leaving the system with a stable periodic solution. Typically, resonator neurons are type II and integrator neurons are type I [1,3,4]

The implications of these different bifurcation structures (Hopf versus saddle-node) go beyond the above-mentioned frequency behavior for type I and II excitability. For instance, the small-amplitude limit cycle present in the subcritical Hopf bifurcation below the transition current originates subthreshold oscillations. Thus, resonator neurons combine oscillatory and excitatory properties close to the bifurcation point and respond preferentially to a given input frequency (show phase locking), while integrator neurons integrate the subthreshold response to a sufficiently high frequency input, do not show subthreshold oscillations, and are more difficult to synchronize.

Real neurons are not purely deterministic devices but usually operate under noisy conditions, due to membrane voltage fluctuations or random synaptic inputs (for an analysis of the sources of neuronal noise, see, for instance, Ref. [5]). The response of individual neurons in the presence of noise has been investigated for a Hodgkin-Huxley model [6] in the context of coherence resonance [7–9]. In analogy to the celebrated stochastic resonance, the coherence of oscillations of an excitable system may be enhanced by a proper amount of noise without any time-periodic input, whenever the system is close to the bifurcation point [8,9]. Other variants of the coherence resonance phenomenon in single element excitable systems have been investigated in the FitzHugh-Nagumo model, which is a simplified version of a resonator

*Electronic address: rgn@imaff.cfmac.csic.es
†Electronic address: gonzalo.polavieja@uam.es

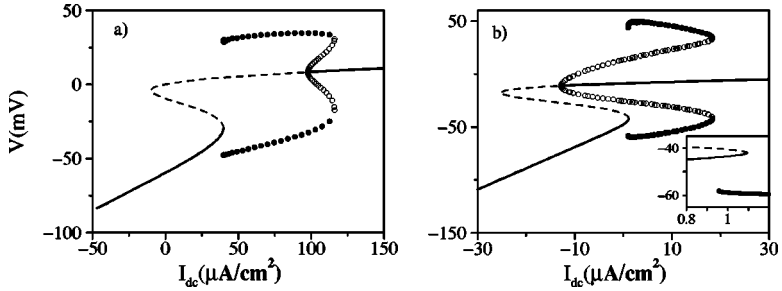

FIG. 1. Bifurcation diagram of the membrane voltage (in mV) as a function of the dc injected current for the two models discussed in the text. (a) Morris-Lecar (Appendix A). (b) Leech neuron (Appendix B). Solid lines: stable fixed points. Dashed lines: unstable fixed points. Filled circles: stable limit cycles. Empty circles: unstable limit cycles. The inset in (b) is an enhancement of the saddle–node bifurcation region showing the coexistence of the stable limit cycle and the node.

neuron [9–13], in models of bursting neurons [14], and in the leaky integrate-and-fire (LIF) neuron model [15]. In the FitzHugh-Nagumo model and a LIF model with absolute refractory period, it has been shown that coherence and anticoherence resonance can be tuned by a proper amount of noise [12,16]. The behavior of a noise-driven dynamical system with a saddle node on a circle bifurcation was studied as one of the first examples of autonomous stochastic resonance [7,8] showing a resonant profile in the signal-to-noise ratio (SNR) of the power spectrum just *below* the bifurcation value. For a recent review on the effects of noise in excitable systems, including coherence and stochastic resonance in some neuron models, see Ref. [17].

Coherence (or its inverse, variability) is usually characterized by the coefficient of variation (CV), defined as the variance to mean ratio in the distribution of interspike intervals (ISI). Variability in ISI distributions of single neurons has important implications for information coding and response reproducibility [18–22]. For neurons with subthreshold oscillations, such as in the Hodgkin-Huxley model, care must be taken with this indicator, since for low noise intensities distributions are multimodal, showing several peaks due to imperfect phase locking between noise-activated spiking and the intrinsic oscillations [11]. Since resonator neurons respond in a narrow frequency range, the correlation time or the SNR of the dominant peak in the power spectrum could be a better measure of the coherence of spiking. Integrator neurons, however, usually show larger coefficients of variation compared to the dominant peak of resonator distributions. This has been shown numerically [23] and analytically [24] for a Θ-neuron model, which corresponds to a one-dimensional normal form of a saddle-node bifurcation. The reason for this higher variability, as we will see, is that ISI distributions of integrator neurons are unimodal and characterized by long exponential tails, due to the broader frequency range of their response. These neurons act, therefore, as Poisson generators and fire with high irregularity.

In this paper, we analyze in detail the spiking features of different realistic models of integrator neurons, under the simultaneous action of a dc current and a noisy input. The coherence as a function of the noise intensity shows a rather different behavior from that of resonator neurons usually investigated in the literature. In particular, when an integrator neuron presents hysteresis (bistability due to coexistence of stable rest and spiking states), the CV may exhibit a maximum as a function of the noise intensity for moderate values of noise level, showing an anticoherence resonance phenomenon. Outside this regime, the CV either decreases or increases monotonically, depending on whether the neuron is before or after the saddle-node bifurcation. We show that for a wide range of noise amplitudes and applied currents, the ISI distributions are of Poisson type, although modified to include a refractory period (spiking with very large frequency is not possible in real neurons due to the recovery time of the membrane potential). The refractory period is important in explaining the bounds for the CV, which is generally less than 1. The anticoherence phenomenon is also well explained by considering two Poisson or renewal processes with different rates, due to the bistable dynamics of the neuron.

I. MODELS AND SPIKING PROPERTIES

We investigate the spiking behavior of two different integrator neuron models, one showing a bistability region and the other without bistability. As a first, simpler case study we use a Morris-Lecar model [25], which is a two-dimensional system originally proposed for the membrane potential of a barnacle muscle fiber. The dynamical variables are the membrane voltage V and the fraction of open potassium channels. The equations and model parameters used are listed in Appendix A. In Fig. 1(a), we show the bifurcation diagram [26] of the membrane voltage as a function of the applied dc current. Stable (unstable) equilibria corresponding to quiescent states are represented by continuous (dashed lines) while stable (unstable) limit cycles corresponding to repetitive firing are shown with filled (empty) circles. For $I \sim 39.95\ \mu A/cm^2$, a saddle-node bifurcation of the fixed point takes place. As anticipated in the previous section, below the bifurcation value three equilibria coexist, one unstable (high voltage) determining the shape of the action potential, another stable (low voltage) which is the rest state, and an unstable saddle point at intermediate voltage acting as a threshold. Since the bifurcation is of the type saddle-node on invariant circle [1,7,27], the limit cycle appears right at the bifurcation point, and thus there is no coexistence of stable rest and spiking sates. Note that a subcritical Hopf bifurcation, rendering the unstable high voltage equilibrium

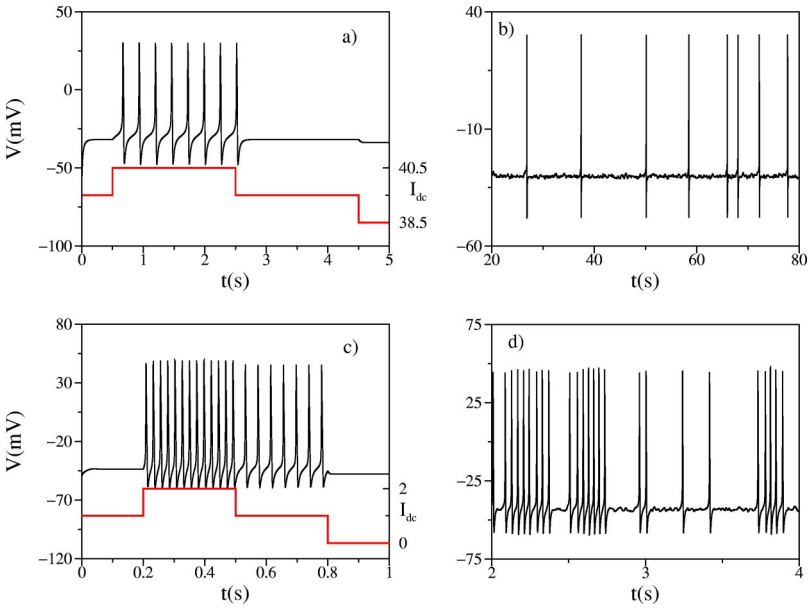

FIG. 2. (Color online) Spiking behavior of the two type I models under a step current and a low intensity noise source in the excitable regime. Top panels: Morris-Lecar. (a) $38.5 \leqslant I_{dc} \leqslant 40.5\ \mu A/cm^2$, $D=0$. (b) $I_{dc}=39.9\ \mu A/cm^2$, $D=0.7$. Bottom panels: leech model. (c) $0 \leqslant I_{dc} \leqslant 2\ \mu A/cm^2$, $D=0$. (d) $I_{dc}=1\ \mu A/cm^2$, $D=0.07$.

stable as the current increases, is also present. However, the bifurcation value is too high to be physiologically relevant.

As another, more realistic instance of an integrator neuron, we have found among experimental research that the spike-generating sodium and potassium conductances of the pressure-sensitive neuron of the leech *Macrobdella decora* [28,29] produce a saddle-node bifurcation of the rest state. The physiological origin of this dynamical behavior is in the potassium conductance; in fact, changing the opening rate for the potassium channel, this model can be converted into a resonator neuron (see Appendix B). The bifurcation diagram for this model is shown in Fig. 1(b). This diagram is very similar to that of Morris-Lecar in the left panel except for two differences: the first one is that the subcritical Hopf bifurcation takes place at negative values of the current. Thus, in all the relevant current range the high voltage quiescent state is stable. This, again, may not be biologically significant for the real neuron since it should be necessary to depolarize the membrane by, for instance, injecting an abnormally high current to artificially place the system in this state. The second difference, more important for the present discussion, is that the stable limit cycle is born in a bifurcation prior to the saddle-node point [see the inset in Fig. 1(b)]. Thus, for a short current interval we have coexistence of a stable rest state and a stable limit cycle. The saddle-node bifurcation takes place at $I_{dc} \sim 1.1\ \mu A/cm^2$, while the limit cycle disappears at $I_{dc} \sim 0.95\ \mu A/cm^2$. The bistable or hysteretic behavior is illustrated in Fig. 2(c) for the deterministic system (no noise) and a step current, where the difference with the Morris-Lecar model [Fig. 2(a)] is apparent. First the neuron is placed in the excitable regime in both cases, close to but previous to the saddle-node bifurcation point. With a sudden increase in voltage of $1\ \mu A/cm^2$, both neurons are brought past the bifurcation point and start periodic firing. After some time, an inhibitory current step brings both systems to the initial current value. In Morris-Lecar [Fig. 2(a)], the system returns to the excitable regime since the limit cycle no longer exists before the saddle-node bifurcation. In the leech neuron [Fig. 2(c)], the system remains in the stable branch of the limit cycle, and continues firing, albeit with lower frequency. Another decrease in current is necessary to hyperpolarize the membrane below the bistability regime and terminate firing. This bistability is also typical of models with a Hopf bifurcation, although the origin is different. As an illustration, we show in Fig. 3 the bifurcation diagram of the modified leech neuron model with resonator properties, and its behavior under a ramp injected current. In this system, the bistability region lies between the Hopf bifurcation point at $I_{dc} \sim 18.3\ \mu A/cm^2$ and the fold limit cycle bifurcation, where the stable and unstable limit cycle collide and disappear, at $I_{dc} \sim 13.6\ \mu A/cm^2$. The most apparent differences in spiking behavior with respect to an integrator neuron are the existence of subthreshold oscillations before and after firing, and the relative insensitivity of the spiking frequency to the intensity of the injected current.

In the rest of the paper, we will add a noisy input I_n to the dc current, which is treated as an Ornstein-Uhlenbeck sto-

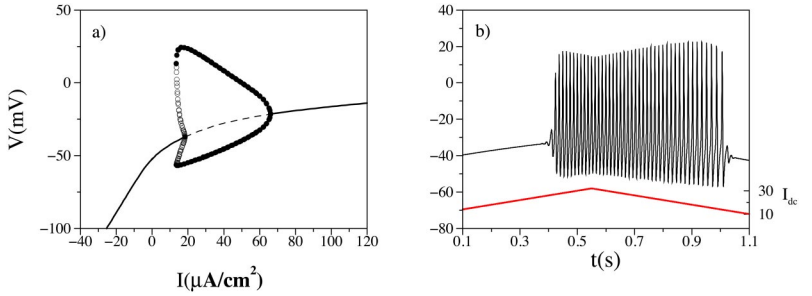

FIG. 3. (Color online) (a) Bifurcation diagram of the leech neuron model shown in Fig. 1(b) with a different closing rate for the potassium channel (see Appendix B). (b) Spiking behavior of the modified leech model under a ramp current.

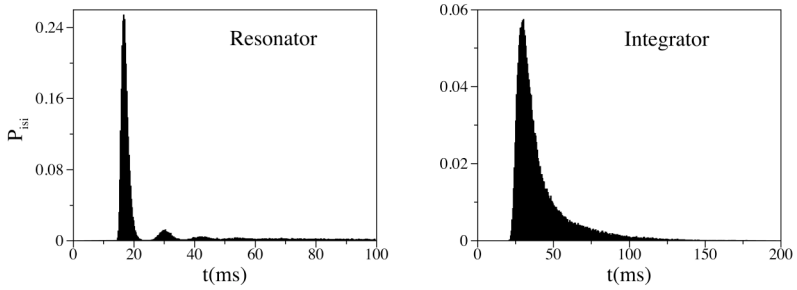

FIG. 4. Interspike interval histograms for a Hodgkin-Huxley model (left) and the leech neuron (right). The noise intensity is the same in both figures, $D=0.7$. The constant current is $I_{dc}=6.5\ \mu\mathrm{A/cm^2}$ for the Hodgkin-Huxley (see Ref. [6]) and $I_{dc}=1\ \mu\mathrm{A/cm^2}$ for the leech model (both neurons are in the bistable regime).

chastic process (Gaussian colored noise). Noisy fluctuations of the membrane voltage with a finite correlation time may be important, for instance, if channel noise (due to the finite number of ion channels in a patch of membrane) or noise due to synaptic transmission are taken into account [5]. The noisy input satisfies the equation

$$\tau\frac{dI_n}{dt} = -I_n + \sqrt{2D}\xi(t), \tag{1}$$

where $\xi(t)$ is a Gaussian white noise, and D and τ are the intensity and correlation time of the stochastic process I_n,

$$\langle I_n(t)I_n(0)\rangle = \frac{D}{\tau}e^{-t/\tau}. \tag{2}$$

In order to separate time scales, we take a correlation time of one order of magnitude less than the relevant period of the system, and thus fix it to $\tau=2$ ms for the leech neuron model and $\tau=20$ ms for the Morris-Lecar model. Nevertheless, we checked that decreasing the correlation time did not affect the statistical quantities, therefore a Gaussian white noise source would produce the same effect on the neuron dynamics.

The spiking behavior of the noise-driven neurons shows qualitative differences in both models, especially for low noise intensities. These are illustrated in Figs. 2(b) and 2(d). In the excitable regime of the Morris-Lecar system ($I_{dc}=39.9\ \mu\mathrm{A/cm^2}$, just below the saddle-node bifurcation value), a low noise intensity produces isolated spikes with very long interspike times between them [compare the time scale in Figs. 2(a) and 2(b)]. Just past the bifurcation value ($I_{dc}=40\ \mu\mathrm{A/cm^2}$), the system fires with regularity and the low noise only modifies slightly the interspike times. On the other hand, if we place the leech neuron in the excitable, but bistable regime ($I_{dc}=1\ \mu\mathrm{A/cm^2}$), firing occurs usually in "bursts" of a few spikes, with long interburst times. Note that inside a burst the firing period is also quite variable. Such a bursting behavior is also present in the Hodgkin-Huxley model in the bistable regime [6], with the difference that inside a burst the firing frequency is very regular and not affected by the noise intensity. Due to its integrator properties, the leech model shows two different noise-induced time scales in the bistable regime: an interburst time, and a time modulating the spiking frequency inside a given burst. As we will see in the next section, these two time scales produce a rather different behavior of the ISI distributions as compared to the Morris-Lecar model.

II. VARIABILITY OF INTERSPIKE TIMES DISTRIBUTIONS

In many cases when experimental recordings are obtained from single neurons, spikes appear as random sequences, even when the external sensory stimuli are held constant [18–21,30]. There are several statistical quantities which are relevant for analyzing information transmission and coding of spiking neurons [31]. Whether the code used by neurons is a "rate code," in which the firing rates of many neurons are averaged to obtain a signal, or a "time code," where the relative times between spikes are meaningful, many important properties can be inferred from the distribution of interspike times. This can be related, for instance, to the distribution of spike counts or to the probability of spiking at a given time [32]. The reliability and precision of spike timing, which plays an important role in information coding of cortical and visual neurons [18–20,22], is also analyzed in terms of ISI distributions and their coefficients of variation. It is thus important to understand properly the dynamical mechanisms by which variability in response to given stimuli arises in single neurons.

As mentioned above, variability as a function of noise has been investigated mainly in resonator neuron models. The subthreshold oscillations may cause phase locking in the bistable regime, where the stable limit cycle and the stable rest state coexist. In the presence of noise, the imperfect phase locking between the interspike intervals and the fundamental period of subthreshold oscillations for certain noise intensities manifests as multimodal ISI distributions with equidistant peaks. This is illustrated in Fig. 4. In the left panel, we show the ISI distribution for a Hodgkin-Huxley neuron model in the bistable regime ($I_{dc}=6.5\ \mu\mathrm{A/cm^2}$, see Ref. [6]) with a noise intensity $D=0.7$. In the right panel, we plot the ISI histogram for the leech neuron model also in the bistable range ($I_{dc}=1\ \mu\mathrm{A/cm^2}$) with the same noise intensity, $D=0.7$. The distribution is unimodal with a larger coefficient of variation than that corresponding to the first peak of the Hodgkin-Huxley model. It has also a long exponential decay typical of a Poisson process (see Fig. 5 and below). This exponential decay is general in ISI distributions of integrator neurons, except for very low noise intensities in the spiking regime (past the saddle-node bifurcation), where the firing frequency is very regular since noise produces a very small effect. In Fig. 5, for instance, we show the ISI distributions for the leech model at large noise intensity ($D=10$, filled circles) and moderate noise ($D=1$, open circles) for $I_{dc}=1\ \mu\mathrm{A/cm^2}$. At this last value, even two different expo-

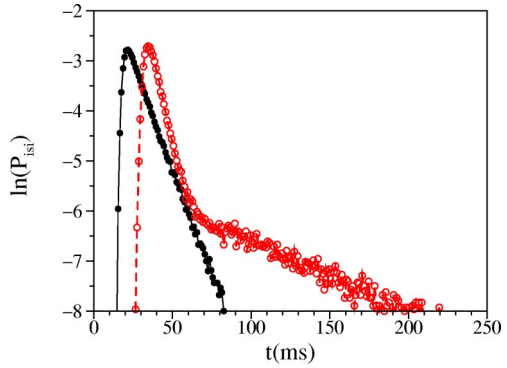

FIG. 5. (Color online) ISI distributions $P_{\mathrm{ISI}}(t)$ for the leech neuron model in the bistable regime ($I_{dc}=1\ \mu\mathrm{A/cm^2}$) at two different noise intensities: $D=0.1$ (empty circles), $D=10$ (filled circles).

nential slopes are clearly visible, which we shall analyze later in more detail. These two time scales are due to the bistable behavior and are never present in the Morris-Lecar model, where only single Poissonian decays are observed in the whole noise range.

In Fig. 6, we show the CV for the Morris-Lecar model as a function of the noise intensity, for a dc current in the excitable regime just before the bifurcation value [$I_{dc}=39.9\ \mu\mathrm{A/cm^2}$, squares; see also Figs. 2(a) and 2(b)] and in the spiking regime ($I_{dc}=40\ \mu\mathrm{A/cm^2}$, circles). The qualitative behavior of the CV is easily understood from the discussion accompanying Figs. 2(a) and 2(b). In the excitable regime, a low noise intensity produces only isolated spikes separated by long interspike times. The firing can be considered as a homogeneous Poisson process with low rate, and ISI distributions are broad and slowly decaying. Increasing the noise intensity increases the rate, and the coefficient of variation decreases. On the contrary, if the neuron is past the bifurcation value, it fires regularly. Noise destroys this regularity and, since spikes can be generated with a broad frequency range, firing can be considered again a Poisson process but now with a high rate, producing higher coherence (smaller CV). As noise increases, coherence is destroyed and the CV also increases.

An important observation is that the CVs are always less than 1, as it should be for a purely Poisson process. This is due to the fact that neurons cannot respond inmediately after a spike but need a refractory time for returning to the rest value of the membrane potential [31]. The simplest way to introduce the refractory period in our approach is considering an inhomogeneous Poisson process [20], where the

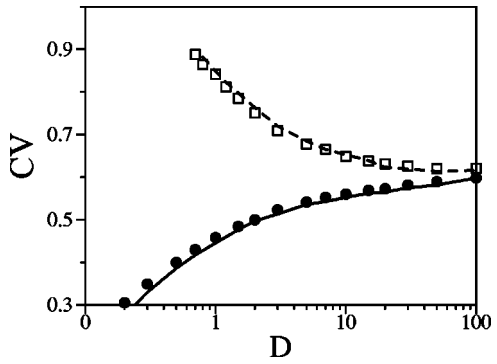

FIG. 6. Coefficients of variation of the ISI distributions for the Morris-Lecar system in the excitable regime ($I=39.9\ \mu\mathrm{A/cm^2}$, open squares) and in the spiking regime ($I=40\ \mu\mathrm{A/cm^2}$, filled circles). The solid and dashed lines are the theoretical prediction Eq. (7) with a power-law dependence for the refractory period $t_0(D)\propto D^{-\gamma}$, $\gamma\sim 0.3$ in both cases, and the rates $\rho_1(D)$ numerically obtained from the ISI distributions (see main text).

probability of spiking in a small interval around time t, $p_s(t,t+dt)$, is proportional to an instantaneous firing rate $r(t)$,

$$p_s(t,t+dt)=r(t)dt. \tag{3}$$

Then the interspike times are distributed according to [32]

$$P_{isi}(t)=e^{-\int_0^t r(t')dt'}r(t). \tag{4}$$

Since we know that at long times spiking is Poisson with constant rate ρ, we approximate the instantaneous rate $r(t)$ by [20]

$$r(t)=w(t)\rho, \tag{5}$$

where $w(t)$ is a recovery function accounting for the refractory time. Note that this function can be obtained numerically from the ISI distribution. The exponential factor in Eq. (4) gives the probability that there is no spike during a time t [31,32], that is, the survival probability $S(t)=1-\int_0^t P_{isi}(t')dt'$. Therefore, the recovery function can be calculated as

$$w(t)=\frac{1}{\rho}\frac{P_{isi}(t)}{S(t)}. \tag{6}$$

This function is nearly zero for small times and increases rapidly at some given time t_0, since $S(t)\to 0$ in a short time interval. For $t\to\infty$, $w(t)=1$, see Fig. 7(a). Therefore, in order to keep the approach analytically simple, we approximate

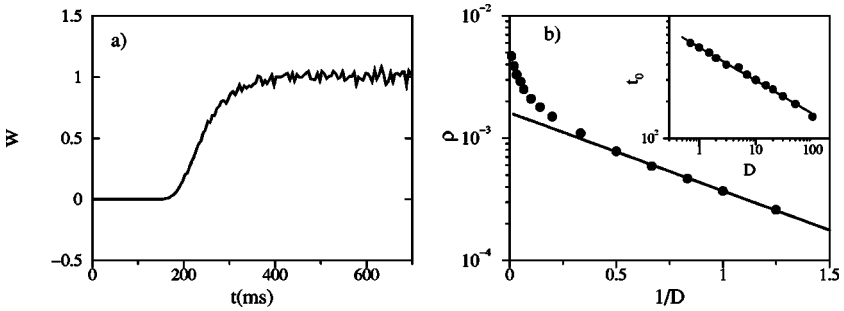

FIG. 7. (a) Recovery function of the Morris-Lecar system in the excitable regime at $D=10$, calculated from the ISI distribution following Eq. (6). (b) Rate ρ and absolute refractory period t_0 (inset) as a function of the noise intensity for the Morris-Lecar model in the excitable regime ($I_{dc}=39.9\ \mu\mathrm{A/cm^2}$).

$w(t)$ by a Heaviside function $w(t)=\theta(t-t_0)$ (absolute refractory period), where t_0 nearly coincides with the maximum of the distribution. We also approximated $w(t)$ by a smooth function, such as a sigmoidal function (relative refractory period), but it did not change significantly the results. With this choice for $w(t)$ it is straightforward to calculate the coefficient of variation for the single Poisson process with ISI distribution (4),

$$CV = \frac{1}{1+\rho t_0}. \tag{7}$$

Note that ρ and t_0 are functions of the noise intensity, but in any case both are positive quantities and the CVs always less than 1 for this simple model. When the system is in the excitable regime, it is tempting to assume an exponential dependence on noise intensity for the rate ρ [9,12], $\rho \propto \exp(-U/D)$, following Kramers' theory of noise–activated rate processes. This means that the transition from quiescence to spiking is equivalent to surmounting an effective barrier U due to random fluctuations, with $U/D \gg 1$. In our case, we observe this exponential dependence for the Morris-Lecar model at $I_{dc}=39.9\ \mu\mathrm{A/cm^2}$ only for $D \leqslant 3$, as shown in Fig. 7(b). If the Kramers' dependence were valid for the whole D range, we would obtain the minimum in CV characteristic of coherence resonance, which is not the case. On the other hand, when looking at t_0 as a function of D we see that it follows rather well a power law (inset of Fig. 7), $t_0(D) \propto D^{-\gamma}$, with $\gamma \sim 0.3$ both in the excitable and spiking regimes. Using this dependence for t_0 and the numerically obtained values for the rate ρ at each noise intensity, we plot in Fig. 6 the theoretical prediction Eq. (7) as a function of D (solid and dashed line). The good agreement confirms the validity of the simple Poisson model with absolute refractory time to predict variability of ISI distributions of integrator neurons *without* bistability, both in the excitable and spiking regimes. We note also that at large noise intensities, the CV tends to a value close to $1/\sqrt{3}$, which is the strong noise limit result for the one-dimensional normal form of a saddle-node system [24].

For an integrator neuron with a bistability region, as the leech model, the behavior of the CV is rather different in this region. In Fig. 8, we show the CV as a function of the noise level for the leech neuron at three different values of the dc current: in the excitable regime, previous to the appearence of the limit cycle ($I_{dc}=0.9\ \mu\mathrm{A/cm^2}$, open squares); in the bistable regime ($I_{dc}=1\ \mu\mathrm{A/cm^2}$, filled circles); and in the spiking regime, after the saddle-node bifurcation ($I_{dc}=1.1\ \mu\mathrm{A/cm^2}$, open triangles). The excitable and spiking regimes are similar to those described for the Morris-Lecar system, and the behavior is well accounted for by the simple Poisson model with absolute refractory time, except at very low noise intensities. On the other hand, for low to moderate noise intensities in the bistable regime, the CV presents a well defined maximum which is characteristic of *anticoherence* [33]. At these noise intensities in this regime, ISI distributions have the double Poisson decay shown in Fig. 5. An intuitive explanation for this behavior can be given following the discussion of Figs. 2(c) and 2(d). For low to intermediate

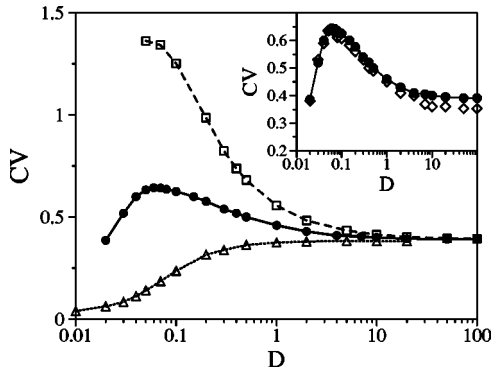

FIG. 8. Coefficients of variation of the leech neuron for three different values of the dc current. Excitable regime, $I_{dc}=0.9\ \mu\mathrm{A/cm^2}$, open squares and dashed line. Bistable regime, $I_{dc}=1\ \mu\mathrm{A/cm^2}$, filled circles and solid line. Spiking regime, $I_{dc}=1.1\ \mu\mathrm{A/cm^2}$, open triangles and dotted line. In the inset, we show with open diamonds the prediction of the two renewals model Eq. (8) with rates, refractory, and crossover times numerically obtained from the ISI distributions.

D, the spikes appear now in bursts as those shown in Fig. 2(d). Now, for low noise, the interburst times are very long and the significant variability is given mainly by the coherence inside a burst, which is large. For intermediate noise, interspike and interburst times are comparable and coherence is minimum (maximum variability in Fig. 8), while for high noise levels we have again a single Poisson process with increasing rate, see Fig. 5, and the CV decreases as in the Morris-Lecar system in the excitable regime.

The ISI distributions in the bistable regime can be formally expressed, using the same approach as above, as

$$P_{isi}(t) = \Theta(t_1-t)\rho_1 w(t) e^{-\rho_1 \int_0^t w(t')dt'} + C\Theta(t-t_1)\rho_2 w(t) e^{-\rho_2 \int_0^t w(t')dt'}, \tag{8}$$

where ρ_1 and ρ_2 give the two different rates, t_1 is the crossover time between the two exponential decays, and $C=\rho_1 \exp[(\rho_2-\rho_1)\int_0^{t_1} w(t')dt']/\rho_2$ imposes continuity at $t=t_1$. For a recovery step function, $w(t)=\Theta(t-t_0)$, the CV can be obtained analytically, although the expression is much more cumbersome than that for the single Poisson process [note that this case is recovered from Eq. (8) for $t_1 \to \infty$]. The absolute refractory period t_0 and the crossover time t_1 follow rather well a power law as a function of the noise intensity, $D^{-\gamma}$, both with exponent $\gamma \sim 0.1$. The rate ρ_2, giving the average interburst frequency, is again an activated process of Kramers' type only for $D \leqslant 0.2$.

In the inset of Fig. 8, we compare the numerical coefficients of variation (filled circles) with those calculated from the distribution Eq. (8) (open diamonds), with rates obtained from the numerical ISI distributions. The maximum appears in the region where both rates contribute significantly to the interspike frequency, confirming our qualitative explanation for the anticoherence behavior in the bistable region.

Finally, it is interesting to investigate if other second-order properties of the stochastic spiking process, such as the

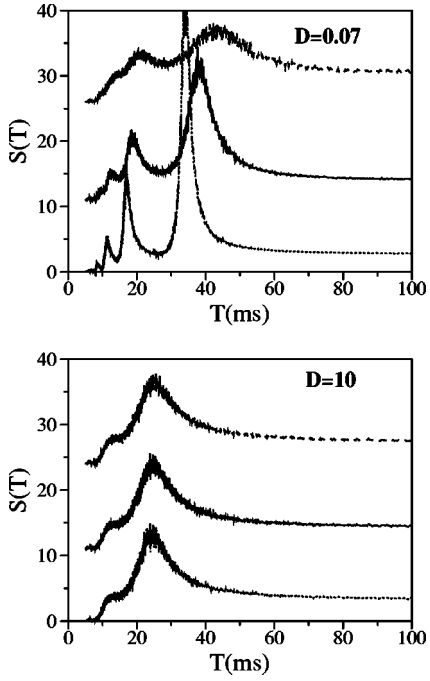

FIG. 9. Power spectra as a function of the period (inverse frequency) for the leech model at two different noise intensities: $D=0.07$ (top panel) and $D=10$ (bottom panel). The top spectrum corresponds in both cases to the excitable regime ($I_{dc}=0.9\ \mu\mathrm{A/cm^2}$), the middle one to the bistable regime ($I_{dc}=1\ \mu\mathrm{A/cm^2}$), and the bottom one to the spiking regime ($I_{dc}=1.1\ \mu\mathrm{A/cm^2}$).

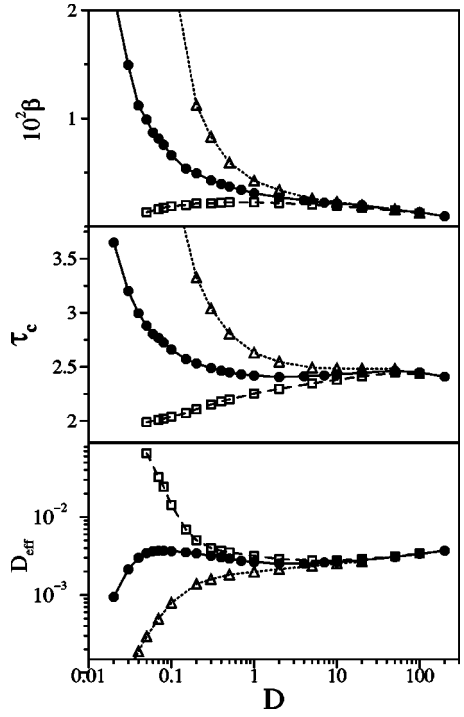

FIG. 10. Signal-to-noise ratio (top), correlation time (middle), and effective diffusion coefficient (bottom) as a function of the noise intensity for the leech neuron model. Symbols are as in Fig. 8: open squares and dashed line, excitable regime, $I_{dc}=0.9\ \mu\mathrm{A/cm^2}$. Filled circles and solid line, bistable regime, $I_{dc}=1\ \mu\mathrm{A/cm^2}$. Open triangles and dotted line, spiking regime, $I_{dc}=1.1\ \mu\mathrm{A/cm^2}$.

power spectrum or the correlation time, also reflect the variability of the ISI distributions as a function of the noise intensity. It is known that a minimum or maximum in the CV does not necessarily imply the same behavior in other indicators, such as spectral coherence [17,34].

First, we see that the power spectra qualitatively reproduce the expected differences in variability in the three regimes. In Fig. 9, we show the power spectra for the leech neuron model at two different noise intensities, $D=0.07$ (around the maximum seen in Fig. 8) and $D=10$. The top spectra were obtained with the neuron in the excitable regime ($I_{dc}=0.9\ \mu\mathrm{A/cm^2}$), the middle ones in the bistable regime ($I_{dc}=1\ \mu\mathrm{A/cm^2}$), and the low spectra in the spiking regime ($I_{dc}=1.1\ \mu\mathrm{A/cm^2}$). The maximum of the dominant peak approximately coincides with the maximum of the ISI distribution. For low and moderate noise intensities, the coherence of the main peak is very different in the three regimes, as expected. At low noise intensity, the neuron fires very regularly in the spiking regime, at nearly the frequency of the limit cycle (the lower intensity peaks in the spectrum corresponding to even and odd harmonics of this frequency), and irregularly in the excitable regime since spikes are isolated by long interspike periods. A strong noise source ($D=10$) makes uniform the coherence of spiking, and the three regimes approximately present the same power spectra. In order to quantify this behavior, we calculate the SNR of the main peak in the power spectrum, defined as usual by

$$\beta = \frac{S(\omega_{max})\omega_{max}}{\Delta\omega}, \tag{9}$$

where $\Delta\omega$ is the full width at half maximum of the peak (the peak is well fitted to a Lorentzian shape, indicating an exponential overall decay of the correlation function). This is shown in the top panel of Fig. 10 for the three different regimes. In the bistable regime (filled circles), coherence decreases faster until $D\sim 1$ where it nearly saturates, although it does not show the minimum characteristic of anticoherence. The correlation time τ_c, defined as the time average of the squared correlation function [9], shows a similar behavior (Fig. 10, middle panel) but it now presents a shallow minimum around $D\sim 1$, indicating a weak anticoherence. Finally, we calculate the effective diffusion coefficient of the spike count distribution $N(t)$ (number of spikes until a time t), which is related to the variance $\langle \Delta T^2\rangle = \langle T^2\rangle - \langle T\rangle^2$ and mean $\langle T\rangle$ of the interspike intervals by [32]

$$D_{eff} = \lim_{t\to\infty} \frac{\langle N^2(t)\rangle - \langle N(t)\rangle^2}{2t} = \frac{1}{2}\frac{\langle \Delta T^2\rangle}{\langle T\rangle^3}. \tag{10}$$

In the bottom panel of Fig. 10 we show the effective diffusion coefficient as a function of the noise intensity obtained from the ISI distribution in the same way as for Fig. 8. It is seen that in the bistable regime (filled circles) it has a maximum at approximately the same value of the CV. In the excitable regime (open squares), dispersion in the spike

count is high at low noise intensities since spikes appear isolated or in bursts of very few spikes, while in the spiking regime (open triangles), firing is very regular and dispersion small at low noise. We remark that in integrator neurons, opposite to resonators, there is not a preferred frequency of spiking even at low noise intensity, and the autocorrelation function does not show the neat oscillatory behvior seen, for instance, in the FitzHugh-Nagumo system in Ref. [9]. Thus, in integrator neurons the CV or the diffusion coefficient are likely more appropriate measures of variability than the correlation time or the SNR.

III. CONCLUSIONS

Noise is an unavoidable ingredient in neurons operating under real conditions. It is argued, however, that some times it may play a useful role in neural computation enhancing detection of weak signals or improving information processing [35,36]. It is thus important to understand the dynamical mechanism of the noise-induced response in single neurons.

In this article we have focused on the response variability to a constant stimulus with noise in neurons close to a saddle-node bifurcation (integrators). Opposite to most usually studied models of resonator neurons, such as the Hodgkin-Huxley or FitzHugh-Nagumo models, the two realistic systems investigated here do not show a coherence resonance behavior in the ISI distributions, although an anticoherence phenomenon is displayed under bistability conditions. These distributions are also very different from those in resonator neurons, which due to the presence of subthreshold oscillations may show phase locking and thus several peaks at integer values of the average interspike period. Integrator neurons fire with higher irregularity and are characterized by a Poisson decay of the ISI distribution even at low noise intensity. This is caused by the much broader frequency range of their response. We have shown that the inclusion of the refractory time is necessary to account for the observed values of coefficient of variation, both in the excitable and spiking regimes, although the different trends at low noise intensities are given by the noise dependence of the Poisson rate. The refractory periods follow a power law as a function of noise in all the cases analyzed. In the bistable region, two different time scales are present. This is due to the peculiar firing features in this region, since spikes are generated mainly in bursts with a large variability in the interburst and interspike times. The interplay between these two time scales maximizes variability if the significant response time is not made arbitrarily large.

Finally, let us mention that many neurocomputational properties depend critically on the underlying dynamics of the neuron [1]. It is known that most models of cortical neurons are integrators, while neurons in invertabrates are typically resonators. The study presented here may help to better understand recent experiments of variability in cortical neurons [19,22,37]. Especially, bistability may play a role in the computational properties of these neurons. In spite of their higher variability, integrator neurons under low and moderate noise intensities may be able to discriminate frequencies in a short range of dc input, and have more flexibility in changing the preferred frequency range than resonator neurons.

ACKNOWLEDGMENTS

This work has been supported in part by DGICYT (Spain) Grants No. BCM2001-2179 and No. BFM2003-06242, and by fBBVA, Spain.

APPENDIX A: MORRIS-LECAR EQUATIONS

Morris and Lecar [25] proposed the following two-variable model of membrane potential for a barnacle muscle fiber:

$$C\frac{dV}{dt} = -g_{\mathrm{Ca}}m_\infty(V)(V-V_{\mathrm{Ca}}) - g_{\mathrm{K}}w(V-V_{\mathrm{K}}) - g_L(V-V_L) + I_{dc},$$

$$\frac{dw}{dt} = \phi[w_\infty(V) - w]/\tau_w(V),$$

$$m_\infty(V) = \frac{1}{2}\{1+\tanh[(V-V_1)/V_2]\},$$

$$w_\infty(V) = \frac{1}{2}\{1+\tanh[(V-V_3)/V_4]\},$$

$$\tau_w(V) = 1/\cosh[(V-V_3)/V_4], \tag{A1}$$

where C is the membrane capacitance, V the membrane voltage, g_{Ca}, g_K, and g_L calcium, potassium, and leakage conductances, respectively, w the fraction of open potassium channels, and I_{dc} the applied dc current. The parameters used are (see Ref. [23]) $C=20\ \mu\mathrm{F/cm^2}$, $g_{\mathrm{Ca}}=4\ \mathrm{mS/cm^2}$, $g_{\mathrm{K}}=8\ \mathrm{mS/cm^2}$, $g_L=2\ \mathrm{mS/cm^2}$, $V_{\mathrm{Ca}}=120$ mV, $V_{\mathrm{K}}=-84$ mV, $V_L=-60$ mV, $V_1=-1.2$ mV, $V_2=18$ mV, $V_3=12$ mV, $V_4=17.4$ mV, and $\phi=0.067$.

APPENDIX B: LEECH P-NEURON EQUATIONS

The spiking activity of the leech *Macrobdella decora* mechanosensory P-neuron (responding to pressure) was found to be produced mainly by a sodium current I_{Na} and a delayed rectifier potassium current I_{K} [28]. The equations and parameters used here are as follows (see Ref. [29]):

$$C\frac{dV}{dt} = -g_{\mathrm{Na}}m^4h(V-V_{\mathrm{Na}}) - g_{\mathrm{K}}n^2(V-V_{\mathrm{K}}) - g_L(V-V_L) + I_{dc},$$

$$\frac{dm}{dt} = \frac{m_\infty(V)-m}{\tau_m(V)},$$

$$\frac{dh}{dt} = \frac{h_\infty(V)-h}{\tau_h(V)},$$

$$\frac{dn}{dt} = \frac{n_\infty(V)-n}{\tau_n(V)}, \tag{B1}$$

where the asymptotic values x_∞ and time constants τ_x are given in terms of the opening and closing rates of the gating variables m, h, n, as in the Hodgkin-Huxley-type equations, by $x_\infty(V)=\alpha_x(V)/[\alpha_x(V)+\beta_x(V)]$ and $\tau_x(V)=1/[\alpha_x(V)+\beta_x(V)]$, with

$$\alpha_m(V) = \frac{0.03(V+28)}{1-e^{-(V+28)/15}},$$

$$\beta_m(V) = 2.7e^{-(V+53)/18},$$

$$\alpha_h(V) = 0.045e^{-(V+58)/18},$$

$$\beta_h(V) = \frac{0.72}{1+e^{-(V+23)/14}},$$

$$\alpha_n(V) = \frac{0.024(V-17)}{1-e^{-(V-17)/8}},$$

$$\beta_n(V) = 0.2e^{-(V+48)/35}. \quad \text{(B2)}$$

Conductances and Nernst potentials have the values $g_{\mathrm{Na}}=350\ \mathrm{mS/cm^2}$, $g_{\mathrm{K}}=6\ \mathrm{mS/cm^2}$, $g_L=0.5\ \mathrm{mS/cm^2}$, $V_{\mathrm{Na}}=60.5\ \mathrm{mV}$, $V_K=-68\ \mathrm{mV}$, $V_L=-49\ \mathrm{mV}$, and $C=1\ \mu\mathrm{F/cm^2}$. For a neuron with resonator properties [presenting only a Hopf bifurcation as shown in Fig. 3(a)], parameters are the same except for the opening rate of the potassium gating variable, $\alpha_n(V)=0.024(V-17)/(1-e^{-(V-17)/18})$.

[1] E. M. Izhikevich, Int. J. Bifurcation Chaos Appl. Sci. Eng. **10**, 1171 (2000).
[2] A. L. Hodgkin, J. Physiol. (London) **117**, 500 (1948).
[3] J. Rinzel and G. B. Ermentrout, in *Methods in Neuronal Modelling: From Synapses to Networks*, edited by C. Koch and I. Segev (MIT Press, Cambridge, MA, 1998).
[4] H. R. Wilson, *Spikes, Decisions and Actions* (Oxford University Press, Oxford, 1999).
[5] A. Manwani and C. Koch, Neural Comput. **11**, 1797 (1999).
[6] S.-G. Lee, A. Neiman, and S. Kim, Phys. Rev. E **57**, 3292 (1998).
[7] W.-J. Rappel and S. H. Strogatz, Phys. Rev. E **50**, 3249 (1994).
[8] H. Gang, T. Ditzinger, C. Z. Ning, and H. Haken, Phys. Rev. Lett. **71**, 807 (1993).
[9] A. S. Pikovsky and J. Kurths, Phys. Rev. Lett. **78**, 775 (1997).
[10] J. P. Baltanás and J. M. Casado, Physica D **122**, 231 (1998).
[11] V. A. Makarov, V. I. Nekorkin, and M. G. Velarde, Phys. Rev. Lett. **86**, 3431 (2001).
[12] A. M. Lacasta, F. Sagués, and J. M. Sancho, Phys. Rev. E **66**, 045105(R) (2002).
[13] A. Zaikin, J. García-Ojalvo, R. Báscones, E. Ullner, and J. Kurths, Phys. Rev. Lett. **90**, 030601 (2003).
[14] A. Longtin, Phys. Rev. E **55**, 868 (1997).
[15] K. Pakdaman, S. Tanabe, and T. Shimokava, Neural Networks **14**, 895 (2001).
[16] B. Lindner, L. Schimansky-Geier, and A. Longtin, Phys. Rev. E **66**, 031916 (2002).
[17] B. Lindner, J. García-Ojalvo, A. Neiman, and L. Schimansky-Geier, Phys. Rep. **392**, 321 (2004).
[18] R. de Ruyter van Steveninck, G. D. Lewen, S. P. Strong, R. Koberle, and W. Bialek, Science **275**, 1805 (1997).
[19] Z. F. Mainen and T. J. Sejnowski, Science **268**, 1503 (1995).
[20] M. J. Berry and M. Meister, J. Neurosci. **18**, 2200 (1998).
[21] T. W. Troyer and K. D. Miller, Neural Comput. **9**, 971 (1997).
[22] M. N. Shadlen and W. T. Newsome, J. Neurosci. **18**, 3870 (1998).
[23] B. S. Gutkin and G. B. Ermentrout, Neural Comput. **10**, 1047 (1998).
[24] B. Lindner, A. Longtin, and A. Bulsara, Neural Comput. **15**, 1761 (2003).
[25] C. Morris and H. Lecar, Biophys. J. **35**, 193 (1981).
[26] We obtained the bifurcation diagram using the code XPPAUT5.85–*The differential equations tool*, by G. B. Ermentrout. www.pitt.edu/bardware.
[27] G. B. Ermentrout, Neural Comput. **8**, 979 (1996).
[28] J. Johansen and A. L. Kleinhaus, Comp. Biochem. Physiol. A **97**, 577 (1990).
[29] S. A. Baccus, Proc. Natl. Acad. Sci. U.S.A. **95**, 8345 (1998).
[30] N. Brenner, O. Agam, W. Bialek, and R. R. de Ruyter van Steveninck, Phys. Rev. Lett. **81**, 4000 (1998); Phys. Rev. E **66**, 031907 (2002).
[31] P. Dayan and L. F. Abbott, *Theoretical Neuroscience* (MIT Press, Cambridge, MA, 2001).
[32] D. R. Cox, *Renewal Theory* (Methuen, London, 1962).
[33] We used ensembles of $\sim 10^5$ spikes to calculate the distributions. For very small noise intensities, there are few spikes with arbitrarily long interspike times contributing to the variance of the distribution, but which are not relevant for information transmission since the response time of a neuron must be finite. Therefore, we impose a cutoff in time ($t \sim 200$ ms) to obtain the statistical properties. For this time, the number of spikes neglected is less than 5% of the total ensemble, and we checked that doubling this cutoff time did not alter qualitatively the statistical properties.
[34] J. W. Shuai, S. Zeng, and P. Jung, Fluct. Noise Lett. **2**, L137 (2002).
[35] D. F. Russell, L. A. Wilkens, and F. Moss, Nature (London) **402**, 291 (1999).
[36] J. S. Anderson, I. Lampl, D. C. Gillespie, and D. Ferster, Science **290**, 1968 (2000).
[37] B. Gutkin, G. B. Ermentrout, and M. Rudolph, J. Comput. Neurosci. **15**, 91 (2003).